Degradation Profiles of Polyester–Urethane (Hydroxylated Polyester/Diphenylmethane Diisocyanate) and Polyester–Melamine (Hydroxylated Polyester/Hexamethoxymethylmelamine) Coatings: An Accelerated Weathering Study

Ramanuj Narayan,[1] D. K. Chattopadhyay,[1] B. Sreedhar,[2] K. V. S. N. Raju,[1] N. N. Mallikarjuna,[3,*] T. M. Aminabhavi[3]

[1]*Organic Coatings and Polymer Division, Indian Institute of Chemical Technology, Hyderabad 500 007, India*
[2]*Inorganic and Physical Chemistry Division, Indian Institute of Chemical Technology, Hyderabad 500 007, India*
[3]*Center of Excellence in Polymer Science, Karnatak University, Dharwad, 580 003 India*

Received 2 October 2004; accepted 17 November 2004
DOI 10.1002/app.21568
Published online in Wiley InterScience (www.interscience.wiley.com).

ABSTRACT: The successful material performance of coatings depends on the environmental conditions to which they are exposed. The effects of the diol structure and acetoacetylation on the weathering degradation of hydroxylated polyester (HP)/hexamethoxymethylmelamine and HP/diphenylmethane diisocyanate clear coatings were studied. The acetoacetylation of HPs led to better performance for higher application solids than the acetoacetylation of their base counterparts. Weathering degradation profiles were investigated with dynamic mechanical thermal analysis, scanning electron microscopy, and X-ray photoelectron spectroscopy. The structural variations of the building blocks and acetoacetylation were found to be important for enhancing the stability of coatings at higher application solids. Polyester–urethane coatings were more stable toward weathering than polyester–melamine coatings. © 2005 Wiley Periodicals, Inc. J Appl Polym Sci 97: 1069–1081, 2005

Key words: coatings; polyesters; degradation; urethane; accelerated weathering

INTRODUCTION

Thermoset melamine and polyurethane (PU) coatings are the most common types of coatings used in aircraft and related industries.[1] During outdoor weathering, such coatings can undergo degradation because of ultraviolet (UV) radiation, water, and oxygen in the atmosphere, and this reduces their service life. In the literature, various accelerated weathering test methods have been reported for studying the weathering-induced degradation of coatings.[2–4] A variety of accelerated weathering test methods have been developed to meet the requirements of rapid growth in new coatings and to achieve improvements over the existing ones. A disadvantage of natural outdoor weathering is that it takes years to obtain meaningful data. However, using accelerated test methods helps to accelerate natural environments with higher stress, such as higher intensity UV radiation and elevated temperatures, without a change in the failure mechanism. Thus, the performance of coating systems can be estimated in a short period. Techniques such as X-ray photoelectron spectroscopy (XPS), scanning electron microscopy (SEM), and differential mechanical thermal analysis (DMTA) can be used to analyze the coating systems.[2,5,6] These techniques are better than traditional methods[7] such as weight loss and gloss loss for the examination of weathered coatings.[7–14]

In the literature, many types of accelerated test methods are reported, ranging from salt spray tests for corrosion resistance to QUV tests and prohesion chambers for resistance to UV and humidity. Changes in the mechanical and physical properties of coatings after accelerated weathering have been compared with dynamic mechanical analysis (DMA) data.[15–17] The degradation of any organic coatings involves chemical breakdown due to photoinitiated oxidation and hydrolysis upon exposure to sunlight, air, and water.[18] Temperature–humidity cycles also affect the durability of coatings. Ranby and Rabek[19] suggested that the photodegradation of PU occurs because of the water-accelerated formation of hydroperoxides in the

This article is CEPS Communication 56.

Correspondence to: K. V. S. N. Raju (drkvsnraju@yahoo.com) or T. M. Aminabhavi (aminabhavi@yahoo.com).
**Present address:* Department of Chemistry, Alan G. MacDiarmid Laboratories for Technical Innovation, University of Texas at Dallas, Richardson, Texas 75080.

Contract grant sponsor: Council of Scientific and Industrial Research.
Contract grant sponsor: University Grants Commission (New Delhi, India).

presence of oxygen. Thus, photoinitiated oxidation produces peroxides, ketones, and aldehydes. The further photooxidation of peroxides and ketones yields peracids, which continue the oxidative degradation as oxidants.[20]

Perrin et al.[21] studied the degradation of acryl urethane and alkyd paints with microattenuated total reflection microspectroscopy. Several different types of mechanisms have been proposed for the photochemical degradation of poly(ether urethane)[22] with Fourier transform infrared (FTIR) spectroscopy. Wilhelm and coworkers[23,24] explained the photooxidation mechanism of urethane segments, whereas Hill et al.[25] studied the short-term accelerated weathering (QUV) of acrylic–melamine topcoats with DMA and concluded that high-melamine coatings displayed greater durability. Biggs et al.[26] studied the weathering durability of exterior polyester–melamine paints by atomic force microscopy (AFM). Skaja and Croll[27] quantified the effects of UV light on a model polyester–urethane coating as it degraded in an accelerated exposure chamber.

Another article of ours[28] deals with the thermal degradation characteristics of polyester–melamine and PU coatings. As a continuation of this work, we now present new experimental results for accelerated weathering. To improve the solid content of the formulation, we carried out 30% acetoacetylation, and we subjected the acetoacetylated coatings to weathering stability evaluation. The replacement of the hydroxyl group with a less polar acetoacetate group increased the solid content at the application viscosity and produced an increase in adhesion because of a chelating effect. The β-ketoester groups were used to modify or crosslink the polymers. The effect of QUV accelerated weathering on the dynamic mechanical properties was evaluated. Finally, a comparison was made between the effects of the diol structure and β-ketoester on the resistance to weathering for both melamine- and isocyanate-based PU coatings. To determine the effects of photodegradation and humidity on the viscoelastic properties of the coatings, we carried out DMTA for samples before and after their exposure to QUV weathering. Changes in the surface morphology of the coatings were investigated with SEM and XPS. The effects of diol and β-ketoester structures on the weathering resistivity of both melamine- and isocyanate-based coatings were investigated.

EXPERIMENTAL

Materials

Neopentyl glycol (NPG) and 1,4-cyclohexane dimethanol (CHDM) from Eastman Chemical Co. (Rochester, NY), trimethylolpropane (TMP) from Aldrich (Milwaukee, WI), 1,3-propane diol (PD) from Lancaster (United States), adipic acid (AA) from SD Fine Chemicals (Mumbai, India), isophthalic acid (IA) from Sisco (Mumbai, India), ethyl acetoacetate (EAA) from Ranbaxy (Mumbai, India), hexamethoxymethylmelamine (HMMM) from Onward Chemicals (Mumbai, India), and polymeric diphenylmethane diisocyanate (MDI) from ICI (Mumbai, India) were used as received.

Synthesis of hydroxylated polyesters (HPs) and casting of coating free films

Three HPs—HP100, HP200, and HP300—with a theoretical hydroxyl value of 240 and with different diol structures were synthesized by the conventional melt condensation technique, as reported previously.[17,28,29] These HPs were trans-acetoacetylated with a stoichiometric amount of EAA to acetoacetylate 30% of the available hydroxyl groups. The resultant acetoacetylated HPs were coded HP103, HP203, and HP303. The melamine-based coatings were formulated with the HMMM crosslinker (the resin/HMMM ratio was 70:30) in the presence of 0.5% *para*-toluene sulfonic acid (*p*-TSA), which was used as a catalyst. These were named by the addition of the letter "M" (e.g., HP100M). PU coatings were prepared via mixing with a stoichiometric amount of MDI and were named HP100MDI, HP200MDI, and HP300MDI, respectively, whereas their acetoacetylated counterparts were named HP103MDI, HP203MDI, and HP303MDI. Free films of these coatings (0.2 mm thick) were prepared via casting onto tin foil, baking at 140°C for 35 min, and amalgamation of the tin substrate. The free films were used for the evaluation of the weathering degradation.

The molecular weights of HPs were determined with gel permeation chromatography (GPC; Shimadzu C-R4A Chro-Topac with Waters 100-Å columns). In this procedure, HP was dissolved in tetrahydrofuran (THF) at approximately 0.01 g/mL, and the experiment was performed at a 1.0 mL/min flow rate with THF as the mobile phase. The columns were calibrated with Aldrich polystyrene standards crosslinked with divinyl benzene. Differential scanning calorimetry thermograms were recorded from −40 to 200°C at a heating rate of 10°C/min under a nitrogen atmosphere at a flow rate of 30 mL/min to determine the glass-transition temperatures (T_g's) of the polyols.

Accelerated weathering of free films

Free films (0.2 mm thick) were fixed on clean and dry panels (Q Panel Co.). Accelerated weathering tests were performed according to ASTM G 53-88 ["Standard Practice for Operating Light and Water Exposure Apparatus (Fluorescent UV-Condensation Type)"] for

TABLE I
Basic Resin Characteristics and Constituents of Base HPs

Property	HP100	HP200	HP300
Constituents	AA, IA, TMP, and NPG	AA, IA, TMP, and CHDM	AA, IA, TMP and PD
M_n	1242	1309	1079
M_w	1913	1549	1825
M_w/M_n	1.54	1.18	1.69
T_g (°C)	−4.3	−33.5	−47.4

M_n = number-average molecular weight; M_w = weight-average molecular weight.

the exposure of nonmetallic materials. In the QUV chamber (Q Panel), fluorescent UV lamps with a peak wavelength of 330 nm were mounted. In the accelerated weathering test, the samples were alternately exposed to UV light for 4 h at 60°C and water-condensed for 4 h at 50°C. This test was conducted for all the samples for 550 h.

DMA

DMA of the unexposed and exposed coating free films was carried out with a DMTA IV instrument (Rheometric Scientific, United States). For the DMTA studies, the specimens were removed from the QUV chamber at different exposure intervals. The DMTA measurements were carried out in a tensile mode at a frequency of 2 Hz, a minimum strain of 0.2%, and a heating rate of 3°C/min. In principle, DMTA examines the viscoelastic behavior of polymers and yields quantitative results for the tensile storage moduli (E'), the corresponding loss moduli (E''), and the loss factor (tan δ) as the quotient of the loss and storage (E''/E'). Here, E' and E'' characterize the elastic and viscous components of the viscoelastic material under deformation.

XPS

The surfaces of a few selected samples and degraded samples were analyzed with a Kratos Axis 165 X-ray photoelectron spectrometer. The X-ray gun was operated at a voltage of 15 kV and at a current of 20 mA. Two types of spectra were collected: a low-resolution spectrum (binding energy = 0–1100 eV) and a high-resolution spectrum of the C1s region (binding energy = 280–300 eV). Survey and high-resolution spectra were collected with pass energies of 80 and 40 eV, respectively. The pressure in the analyzer chamber was approximately 10^{-8} Torr. A thin film (0.2 mm thick) was used for the XPS analysis. The sample was tilted in such a way as to change the angle (θ) between the normal to the sample and the analyzer. At $\theta = 0°$, the sample was perpendicular to the detector, and this led to the maximum sampling depth.

The effective sampling depth (z) was derived with $z = 3\lambda \cos \theta$, where λ is the effective mean free path for electrons to escape the surface, which was set to 2.5 nm. Therefore, at $\theta = 0°$, z was 7.5 nm, and at $\theta = 45°$, z was 5.3 nm.[30] Peak fitting and presentation output were produced with an integrated VISION control and information system. All spectra were presented as charge-balanced and energy-referenced to C1s at 284.6 eV. To determine the types of carbon bonds present, the chemical-bond analysis of carbon was performed via the curve fitting of the C1s peak from high-resolution spectra and its deconvolution.

Surface morphology

The surface morphology of the coating films was investigated with SEM of thin films mounted on aluminum stubs with a double-sided adhesive tape coated with gold. A Hitachi S520 scanning electron microscope was used at an accelerated voltage of 10 kV.

RESULTS AND DISCUSSION

The molecular weights and polydispersities of HPs are reported in Table I. The estimation of the molecular weights of low-molecular-weight oligomers by GPC is often unreliable, presumably because of changes in the retention volumes of oligomeric species. The higher molecular weight of HP200, with respect to that of HP100, could be attributed to the esterification rate of CHDM being higher than that of NPG. Thus, the difference in polyesterification was due to greater steric crowding of the NPG moieties. The low molecular weight of HP300 was due to concurrent sluggishness of the very low-molecular-weight oligomers for building up large polymer chains. Upon acetoacetylation, there was a gradual decrease in the molecular weights of HPs (data not tabulated), probably because of a breakdown or scrambling of the polyester backbone upon acetoacetylation. This type of reduction might be accompanied by the capping of the polyester with an ethyl alcohol coproduct from EAA, as reported earlier.[31] The polydispersity increased with the increasing acetoacetylation of HPs.

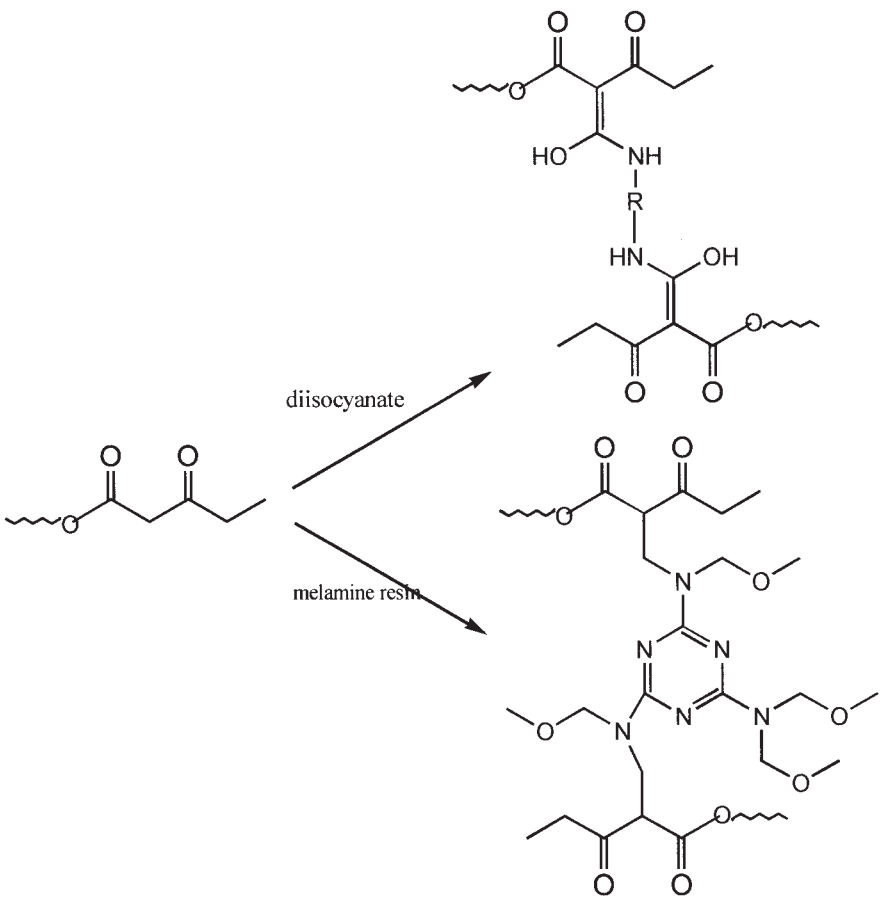

Scheme 1 Crosslinking reaction of the acetoacetate group with diisocyanates and melamine.

The crosslinking reactions in polyol–diisocyanate coatings differ considerably from polyol–melamine crosslinking. This produces differences in the chemistry between the two coating systems that are responsible for the differences in the degradation patterns. The main crosslinking reaction in isocyanate–polyol coatings is the reaction between isocyanate and hydroxyl groups, which forms a urethane crosslink. The other possible reactions are the formation of urea, biuret, and allophanate. The importance of side-product formation depends on the polarity of the resin, the level and type of the catalyst, and the humidity level during crosslinking. In contrast to the fairly simple crosslinking chemistry in urethane coatings, crosslinking in melamine coatings is quite complex because they produce polymer–melamine/melamine–melamine crosslinks or interconvert functional groups.[32,33] The importance of different reactions depends on the catalyst level, the structure, and the baking conditions. For acetoacetylated coatings,[31,34] the crosslinking reaction is still complex because of the involvement of active methylene groups in the β-ketoester moiety, as shown in Scheme 1.

Weathering degradation

In the majority of QUV accelerated weathering experiments, coatings degrade via hydrolytic and photodegradation mechanisms. Analyses of degraded products have been carried out through the photooxidation of coatings with various controlled irradiation instruments.[35,36] Yang et al.[15] studied the blistering and degradation of PU coatings under different accelerated weathering conditions to analyze degraded samples by AFM and SEM, and they showed that QUV exposure was more damaging. Nguyen et al.[37] studied the effect of the relative humidity on the moisture-enhanced photolysis of acrylic–melamine coatings. The degradation of melamine-based coatings in the presence of moisture, UV, and oxygen is very complex. Bauer and a coworker[32,33] suggested that crosslinking reactions in melamine and hydroxy-functional resins are reversible. Thus, melamine-based coatings are susceptible to degradation during outdoor weathering. They also found that the rate of hydrolysis in the presence of UV light is greater than the sum of dark hydrolysis and photolysis. However, the most important features of degradation are changes that result in a loss of initial physical proper-

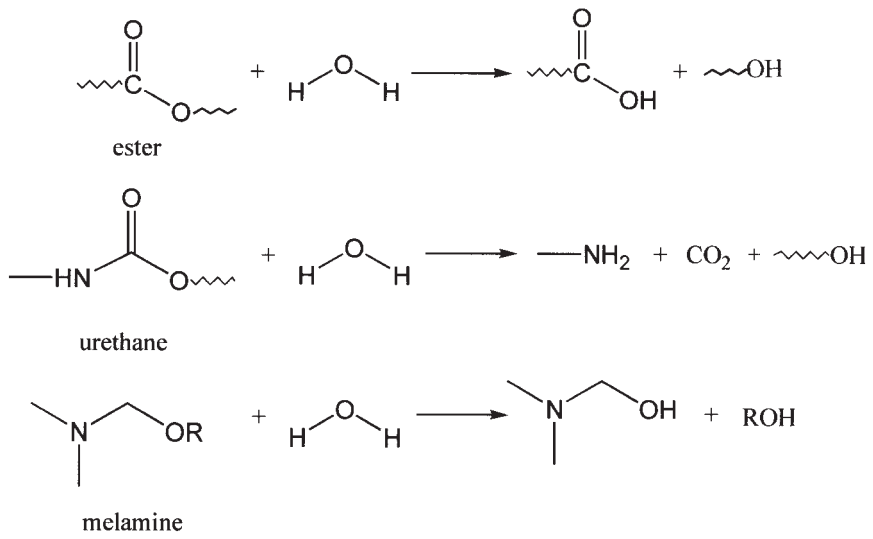

Scheme 2 Hydrolytic breakdown of the polymer matrix (hydrolysis takes place at ester, urethane, and polyester–melamine bonds through the nucleophilic attack of a water molecule).

ties, discoloration, or a lack of adhesion that eventually causes a loss of product integrity for any good use. The exposure of coatings for short periods might result in a very little visible deterioration, such as gloss or yellowing, so more rapid tests are required. Thus, physical methods are useful for investigating changes in the morphology of the composition after exposure. The hydrolytic breakdown of the polymer matrix is shown in Scheme 2.

Visual observations

The yellowness of the PU coatings increased with an increase in the extent of exposure of all the PU films to QUV. This was more pronounced for up to 250 h of exposure. The reason for this difference is a well-recognized observation associated with aromatic diisocyanate-based PU coatings.[38] However, no appreciable surface defects could be observed visually. For HP–HMMM coatings, no appreciable color change was seen during the exposure, but HP303M became very brittle after 250 h; therefore, it was difficult to use the film for further evaluation.

Dynamic mechanical properties

DMTA experiments were conducted on periodically exposed films and on films before exposure. Figures 1 and 2 present plots of E' versus the temperature for exposed HP100MDI and HP103MDI PU coatings. The DMTA data could be correlated with the mechanical properties of the coatings. E' is the elastic part of the dynamic mechanical properties and is related to the stiffness. The length between the glassy and rubbery plateaus represents the flexibility of the coatings. The rubbery plateau modulus (temperature $> T_g$) has a direct relationship with the crosslinking density (ν_e). The E' values in the rubbery region (temperature $> T_g$) were used to calculate ν_e:

$$\nu_e = E'/3RT \quad (1)$$

where R is the molar gas constant and T is the temperature (K).

Figures 1 and 2 show that with increasing exposure time, the coatings became less flexible or more brittle, and ν_e also increased considerably. T_g was taken as the temperature at which tan δ was maximum, and these values are reported in Tables II and III, respectively. The breadth and height of the tan δ curves were used

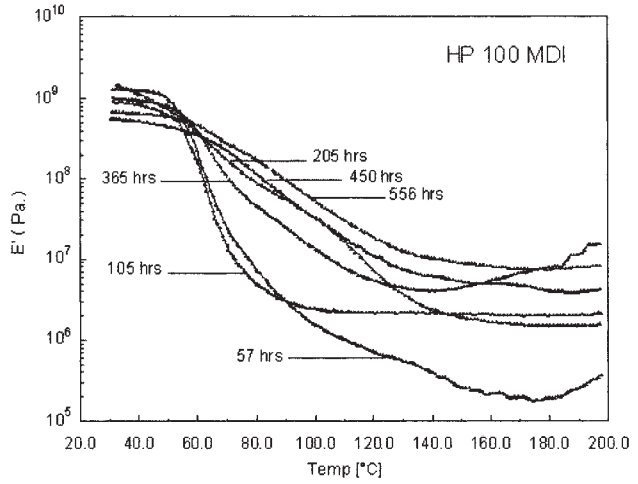

Figure 1 Plot of E' versus the temperature for exposed HP100MDI coatings.

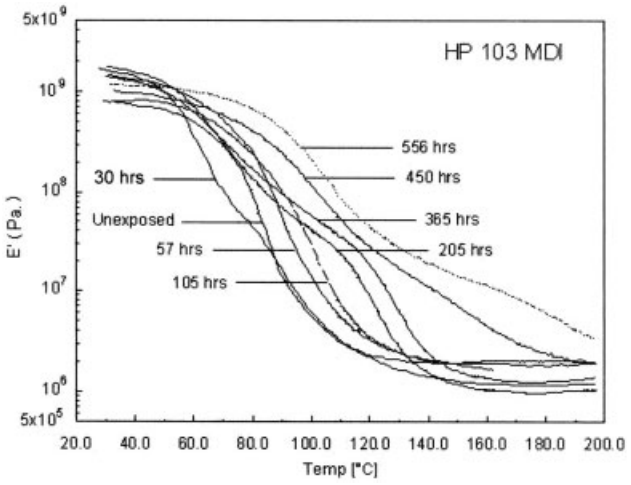

Figure 2 Plot of E' versus the temperature for exposed HP103MDI coatings.

to correlate the flexibility, brittleness, and ν_e values of the coatings. Plots of tan δ versus the temperature for exposed HP200MDI and HP203MDI coatings are shown in Figures 3 and 4, respectively. With one or two exceptions, the height of tan δ decreased, whereas the breadth increased, with the exposure time. The width of the tan δ peak (peak width), expressed as the temperature interval and determined as the height of tan δ_{max} divided by two, increased with the exposure time (data not given).[39,40] The increase in ν_e with the exposure time may have been due to extra crosslinking arising from photooxidation or a temperature scan of DMTA, as generally can happen with ambient-cured coatings. All PU coatings of this study showed similar behavior. A decrease in T_g for unweathered HP100MDI coatings from 83 to 71.2°C was observed after 57 h of weathering. T_g increased and reached 87.5°C after 556 h of weathering, whereas ν_e increased from 2.45×10^{-5} (after 57 h) to 84.6×10^{-5} mol/cm^3. The T_g and ν_e values of the corresponding acetoacetylated coatings (HP103MDI) before weathering and af-

TABLE II
T_g and E' Values of Exposed and Unexposed PU Coatings

System	T_g (°C)	E' (Pa) × 10^{-6} 150°C	$\nu_e \times 10^5$ (mol/cm^3)	System	T_g (°C)	E' (Pa) × 10^{-6} 150°C	$\nu_e \times 10^5$ (mol/cm^3)
HP100MDI (57 h)	71.2	0.26	2.45	HP103MDI (0 h)	84.0	1.9	18.0
HP100MDI (105 h)	82.0	2.1	19.9	HP103MDI (57 h)	85.2	1.8	17.0
HP100MDI (205 h)	83.6	1.85	17.5	HP103MDI (105 h)	89.5	1.9	18.0
HP100MDI (365 h)	85.6	4.46	42.3	HP103MDI (205 h)	89.0	1.18	11.2
HP100MDI (450 h)	86.0	5.3	50.2	HP103MDI (365 h)	95.6	1.6	15.2
HP100MDI (556 h)	87.5	8.93	84.6	HP103MDI (450 h)	96.4	7.1	67.3
HP 200MDI (57 h)	82.8	2.8	26.5	HP103MDI (556 h)	110.2	13.7	130
HP200MDI (105 h)	85.9	5.6	53.1	HP203MDI (57 h)	84.6	7.43	70.0
HP200MDI (153 h)	88.1	5.7	54.0	HP203MDI (153 h)	88.5	8.65	82.0
HP200MDI (205 h)	90.7	8.51	80.7	HP203MDI (365 h)	89.1	14.1	134
HP200MDI (365 h)	95.9	13.2	125	HP203MDI (450 h)	94.0	19.0	180
HP200MDI (450 h)	99.9	14.5	137	HP303MDI (57 h)	73.0	3.18	30.0
HP200MDI (556 h)	101.4	20.4	193	HP303MDI (105 h)	81.6	7.3	7.0
HP300MDI (105 h)	71.0	0.94	8.9	HP303MDI (153 h)	80.9	30.8	292
HP300MDI (153 h)	77.4	—		HP303MDI (200 h)	78.2	1.6	15.2
HP300MDI (205 h)	78.0	1.6	15.2	HP303MDI (356 h)	92.2	6.65	63.0
HP300MDI (365 h)	70.9	6.57	62.3	HPMDI (450 h)	84.1	3.2	30.3
HP300MDI (450 h)	71.9	34.8	330	HP303MDI (556 h)	101.2	3.3	31.3
HP300MDI (556 h)	77.7	7.83	74				

TABLE III
T_g and E' Values of Exposed and Unexposed Polyester–Melamine Coatings

System	T_g (°C)	E' (Pa) × 10^{-6} 150°C	$\nu_e \times 10^5$ (mol/cm^3)	System	T_g (°C)	E' (Pa) × 10^{-6} 150°C	$\nu_e \times 10^5$ (mol/cm^3)
HP100M (0 h)	80.9	1.3	12.3	HP103M (0 h)	65.0	1.53	14.5
HP100M (153 h)	130.2	25.8	245	HP103M (57 h)	78.5	4.74	44.9
HP100M (450 h)	148.1	62.6	593	HP103M (205 h)	79.0, 176	24	228
HP200M (0 h)	81.0	1.97	18.7	HP103M (365 h)	78.0, 156	47.2	447
HP200M (365 h)	94.1	66	625	HP103M (450 h)	75.8, 164.4	96	910
HP200M (556 h)	95.0, 149.7	162	1535	HP203M (0 h)	85.0	28.5	270
HP300M (0 h)	44.23	7.4	70.1	HP203M (105h)	96.2	55.4	525
HP300M (450h)	167.6	218	2066				

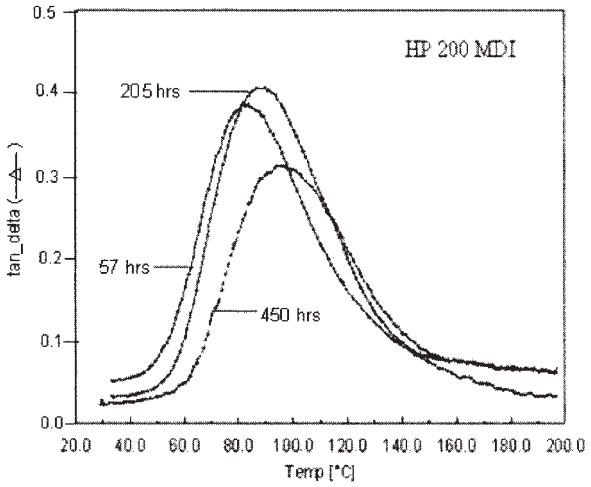

Figure 3 Plot of tan δ versus the temperature for exposed HP200MDI coatings.

ter 556 h of weathering were 84°C and 18.0 × 10^{-5} mol/cm^3 and 110.2°C and 130.0 × 10^{-5} mol/cm^3, respectively. For HP200MDI coatings, T_g and ν_e after 57 and 556 h of weathering were 82.8°C and 26.54 × 10^{-5} mol/cm^3 and 101.4°C and 193.35 × 10^{-5} mol/cm^3, respectively.

The anomalous behavior with the exposure time, as shown in Table II, could be due to different types of degradation mechanisms operating in the presence of UV/H_2O and to other physical processes associated with it. The unstable nature of room-temperature-cured PU films and the nonuse of UV stabilizers in the coating formulation might have caused the facile destruction of urethane bonds. Hill and Kozlowski[40] proposed that a change in T_g could be due to polar groups formed by photooxidation and that chain ends may be preferentially removed during exposure. Gardette and Lemaire[41] proposed a photodegradation mechanism for aromatic diisocyanate-based PUs. The photodegradation of the urethane linkage in aromatic diisocyanate-based PUs proceeds via two mechanisms. At short wavelengths (<340 nm), photolysis proceeds through a photo-Fries reaction. In the presence of oxygen, the oxidation of urethane hard segments occurs in MDI-based PU. This reaction involves radical attack on the central methylene carbon of aromatic structures with the subsequent formation of hydroperoxides, and this leads to the formation of quinone–diimide structures as well as benzoic acid groups. Scheme 3 shows some possible reactions due to the UV degradation of the urethane segment.

Yang et al.[2] proposed a cyclic mechanism for the degradation of PU coatings exposed to UV/H_2O. On the basis of attenuated total reflection/FTIR studies, they showed that the onset of chain scission and reassociation can lead to different conformational changes on the coating surface. Furthermore, upon QUV exposure, chain scission occurs, and because of condensation within the QUV chamber, carbamic acid is formed. However, because of the instability of carbamic acid, carbon dioxide evaporates from the surface. Chain scissions can occur in the soft segments of PU upon exposure, whereas chain scission and reassociation can occur in hard segments. As the UV intensity decreases significantly with the penetration depth, a diminished chain scission of urethane groups occurs in the bulk of the coatings.[42] Upon UV exposure, surface species can be oxidized, and this leads to the formation of carbonyl groups. Here, the physical state of the polymer is important; it controls the magnitude of photodegradation. The network structure must also be considered to study the extent of photodegradation of urethane segments.[32,36,37] On the basis of this evidence and the formation of different intermediates as well as degradation products during the QUV exposure of PU, intermediates and products might have affected the network degradation. Some intermediates that formed might have helped with the formation of crosslinks and the destruction of network at different exposure times. This could be the reason for the observed anomalous behavior.

Figures 5 and 6 display plots of E' versus the temperature and tan δ versus the temperature, respectively, for HP200M coatings before and after exposure to QUV. The dynamic mechanical properties are reported in Table III. The increase in E' of the unexposed polyester–melamine films after 140°C was due to further crosslinking during the DMTA scan. As described earlier,[17] we had to optimize the curing conditions of the melamine-based coatings because of the wide range of the curing zone. Because we optimized the curing conditions at 140°C, the increase in the modulus after this temperature was quite expected. In general, after exposure to alternating (cyclic) UV radiation

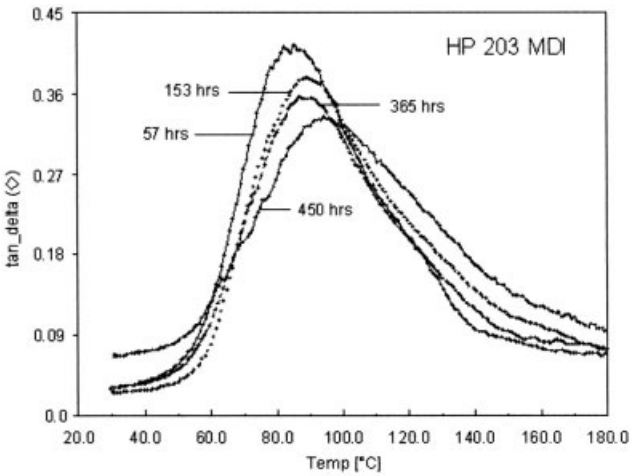

Figure 4 Plot of tan δ versus the temperature for exposed HP203MDI coatings.

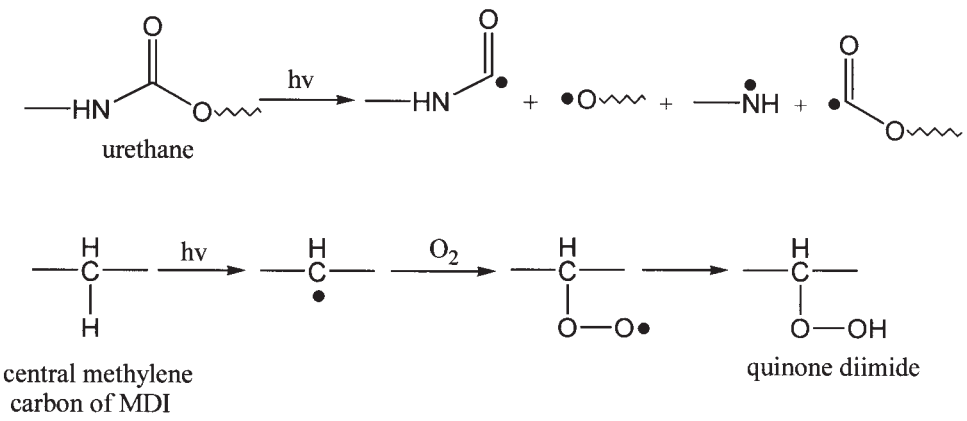

Scheme 3 Photodegradation of the urethane segment in PU.

and water condensation, there was an increase in the rubbery modulus for all the coating films because of further crosslinking reactions.

For HP100M melamine coatings, T_g and ν_e were 80.9°C and 12.3 × 10^{-5} mol/cm^3, respectively. These were changed to 148.1°C and 593 × 10^{-5} mol/cm^3, respectively, after 450 h (see Table III). However, the corresponding acetoacetylated system (HP103M) showed a lower T_g of 65°C, which may have been due to the reduction in the molecular mass of polyester HP103 in comparison with that of HP100, as reported elsewhere.[28] With the progress of degradation, the height of the tan δ curve decreased, and T_g changed considerably for HP103M. After 205 h, two T_g's were observed (see Figs. 7 and 8). The second T_g could be due to a change in or degradation of the melamine distribution due to the formation of a two-layered structure. ν_e was changed from 14.5 × 10^{-5} to 910 × 10^{-5} mol/cm^3 after 450 h of weathering degradation. The change in ν_e was more pronounced with the melamine-based systems than with the corresponding PU coatings. Therefore, in comparison with PU, the melamine-based coatings showed more susceptibility to degradation, as shown by the DMTA data given in Table III.

In general, T_g was higher for exposed films than unexposed films, but tan δ_{max} and peak width values maintained the decreasing and increasing trends, respectively, with the exposure time (Fig. 8 for HP300MD1 coatings). E' at 140°C exhibited the same increasing trend (except for one or two deviations) upon exposure at periodic intervals. The anomalous behavior of the dynamic mechanical properties was also seen in these coatings after different periods of exposure to UV, but it was less pronounced than that in the PU coatings. The degradation of melamine-based coatings in the presence of moisture, UV, and oxygen presents a very complex picture. The net result of the exposure of a melamine crosslinked film is due to the scission of polymer–melamine crosslinks and the formation of melamine–melamine crosslinks, which produces brittleness.[13,32] A mechanism involving free-radical attack on the crosslink and resulting in

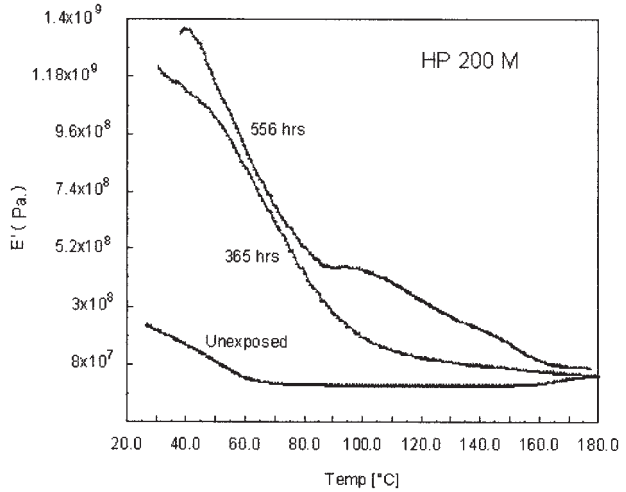

Figure 5 Plot of E' versus the temperature for exposed HP200MDI coatings.

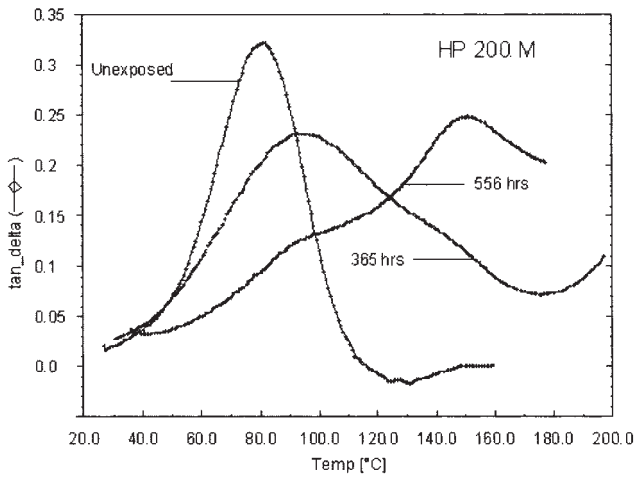

Figure 6 Plot of tan δ versus the temperature for exposed HP200MDI coatings.

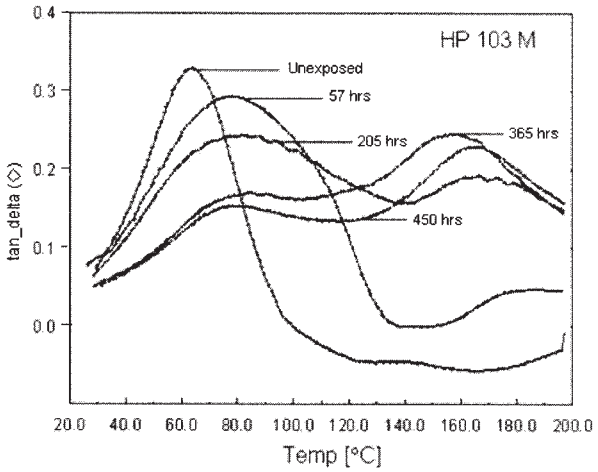

Figure 7 Plot of tan δ versus the temperature for exposed and unexposed HP103MDI coatings.

an —N═CH_2 intermediate during exposure to UV light was proposed by Gerlock et al.[43] In the presence of water, —N═CH_2 hydrolyzes to form a methylol group, and this results in melamine–melamine crosslink formation. Therefore, the scission of both methoxy and polymer–melamine crosslinks occurs at an accelerated rate in the presence of UV light. However, some scissions occur in the absence of water because of a free-radical attack on the crosslinked structure.[44,45]

Now we look at an analysis of the changes taking place during degradation. An increase in E' at 140°C and T_g could be attributed to the self-condensation of melamine and the coupling of free radicals generated by photolytic reactions. The observed anomalous behavior in some cases may be attributed to the fastness or slowness of the reactions, as explained before. For some polyester–melamine coatings, we observed two tan δ peaks, which may have been due to the differences in the layered structures of the films upon exposure. High T_g values were due to highly oxidized and crosslinked outer layers, but low T_g's were due to the bulk layer. Even though UV radiation has the capability of penetrating a polymer sample, the number of photon strikes on the surface of the polymer backbone may not necessarily be the same as that in the bulk. For obvious reasons, the bulk of a polymer will degrade to a lesser extent than the outer surface. Another cause of lesser photooxidation inside the bulk of a sample may be a reduced concentration of molecular oxygen.

The variation of the diol structure in the HP backbone and the modification of the pendant hydroxyl group with the acetoacetyl group resulted in different molecular weights and T_g's. The T_g values of different coating films followed this sequence for both PU and polyester–melamine coatings: HP300 < HP100 < HP200. The use of straight-chain PD (HP300 and HP303) resulted in more flexible coatings, whereas the rigid structure of CHDM increased the T_g values of the HP200 and HP203 series because of interchain stiffness. The structural difference between NPG and PD is the presence of two methyl groups on carbon number 2 of PD. This might have restricted the soft-segment mobility and resulted in higher T_g values. The HP200M coatings were expected to have higher ν_e values because of the diol structure, whereas the HP203M and HP303M coatings were due to acetoacetylation. The HP300M coatings degraded more than the HP100 and HP200 coatings. It is, however, difficult to draw a conclusion on the effect of acetoacetylation on the change in the weathering stability because of the similar types of degradation behaviors. If this is true, then it is useful to acetoacetylate the available hydroxyl groups to reduce hydrogen bonding to make high-solid coatings with improved properties.

XPS

A low-resolution scan was run to determine the percentages of elements present at the surfaces of PU and polyester–melamine films. Relative elemental compositions of the analyzed samples are given in Table IV. The main elements detected by XPS were oxygen and carbon. However, small amounts of nitrogen and tin were also present because of the casting of the samples on tin foil. To better understand the chemical reaction that occurred on the coating surfaces, XPS was used for a surface analysis of the clear coatings. For the HP200MDI and HP203MDI coatings, with an increasing takeoff angle (i.e., toward the surface), the atomic nitrogen percentage decreased. Because the source of nitrogen was MDI and in the PU coatings it was

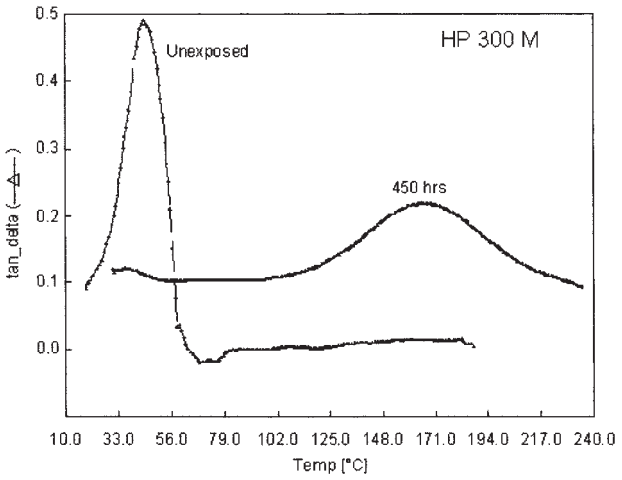

Figure 8 Plot of tan δ versus the temperature for exposed and unexposed HP300MDI coatings.

TABLE IV
Surface Composition (atom %) of Unexposed and Exposed Coatings by AR–XPS at 0 and 45° Takeoff Angles

System	θ (°)	C	O	N
HP200MDI (unweathered)	0	79.62	12.84	7.54
	45	81.22	14.72	4.06
HP203MDI (unweathered)	0	76.81	16.91	6.28
	45	79.28	17.48	3.23
HP203MDI (weathered; 556 h)	0	76.54	20.17	3.29
	45	75.62	18.34	6.04
HP200M (unweathered)	0	82.33	14.23	3.44
	45	77.29	18.63	4.08
HP203M (unweathered)	0	66.51	28.8	4.69
	45	70.84	25.64	3.52
HP203M (weathered; 556 h)	0	65.62	33.72	0.66
	45	69.17	30.31	0.52

associated with urethane bonding, the urethane concentration decreased toward the coating/air interface as a result of more surface energy. The XPS data showed that after 556 h of exposure for HP203MDI coatings, the atomic nitrogen percentage at 45° increased from 3.23 to 6.04, whereas it decreased at 0° (i.e., toward the bulk). This suggests that after 556 h of weathering, the PU coating/air interface was enriched with the urethane/urea content.

It is useful to study the distribution of melamine in polyester–melamine films because it influences and controls ν_e, T_g, structural heterogeneity, and so forth. The distribution of melamine was influenced by factors such as the hydroxyl number of polyester, the type and amount of the acid catalyst, the film thickness, and the curing condition.[46–48] The presence of nitrogen at the polyester–melamine film/air interface was considered an indication of the presence of HMMM because the only source of nitrogen in the polyester–melamine films was HMMM. The atomic nitrogen percentage of the HP200M coatings (see Table IV) increased from 3.44 to 4.08 as the takeoff angle increased from 0 to 45° (i.e., toward the surface, the HMMM concentration was greater). Because the surface composition of the polyester–melamine coatings was dependent on the difference in the free energy between polyester and melamine[49] and HMMM had lower surface free energy, we expected the surface enrichment of melamine to occur. However, the reverse trend of nitrogen distribution with the film depth was observed for unweathered and weathered samples of HP203M. In fact, a reduction in the atomic nitrogen percentage at the coating/air interface was observed for the weathered polyester–melamine films, in comparison with that of the corresponding unweathered coatings.

A high-resolution scan was conducted in the C1s region for each unexposed sample and for each sample weathered for 556 h to determine the types and number of carbon–oxygen bonds present. XPS spectra were recorded at takeoff angles of 0 and 45°. For PU coatings, the C1s peak was deconvoluted into three subpeaks, C—C/C—H, C—O, and C═O, which appeared at 284.6, 285.6–286, and 288.8–289.2 eV, respectively. The corresponding plots and deconvolution peaks for the unexposed HP200MDI and HP203MDI coatings are displayed in Figures 9. Figure 10 shows the deconvoluted spectra of weathered (for 556 h) HP203MDI films at takeoff angles of 0 and 45°, respectively. Because the contribution of the C═O subpeak in the deconvoluted spectra of the PU coatings was due to the ester group of polyester and the urethane group, and if we suppose that the distribution of polyester was uniform with the sample depth, then the ratio of C═O/C—C can be used to interpret the segregation behavior of the urethane component with the coating depth. For the HP200MDI coatings, the C═O/C—C ratios at 0 and 45° were 0.076 and 0.048, respectively, and this suggested that the urethane content preferentially resided toward the bulk of the coatings. Similar observations were made for other PU coatings.

The deconvoluted angle-resolved (AR)–XPS spectra of the unweathered melamine HP200M and HP203M coatings at takeoff angles of 0 and 45° are shown in Figure 11, whereas Figure 12 presents the deconvoluted AR–XPS spectra of weathered (for 556 h) melamine HP203M coatings at takeoff angles of 0 and 45°, respectively. For polyester–melamine coatings, the C1s peak was deconvoluted into four subpeaks, C—C/C—H, C—O, C—N, and C═O, which appeared at 284.6, 285.3–286, 286.2–287.2, and 288.2–288.9 eV, respectively. In the XPS peak, C—N came from HMMM, whereas C═O originated from polyester. Therefore, the ratio of the integration of these peaks could be considered for the quantitative determination of the melamine distribution with the sample depth and with the weathering degradation. For the HP200M coatings, the C—N/C═O ratios at 0 and 45° were 0.836 and 1.227, respectively, and this suggested the surface segregation behavior of melamine toward the coating/air interface because of its lower surface energy. For unweathered HP203M coatings, the C—N/C═O ratio at 0° was 1.579, whereas for HP203M, the weathered (556 h) coatings had C—N/C═O ratios of 0.653 and 1.873 at 0 and 45°, respectively. Therefore, a substantial decrease in the nitrogen concentration was observed at 0° for the HP203M coatings after 556 h of weathering.

Surface morphology

SEM images of the representative PU and polyester–melamine HP200 coating films before and after accelerated exposure for 556 h are shown in Figure 13. The phase images of the PU coatings before degradation show a uniform surface. The surface degradation of the PU coatings after exposure for 556 h is also dis-

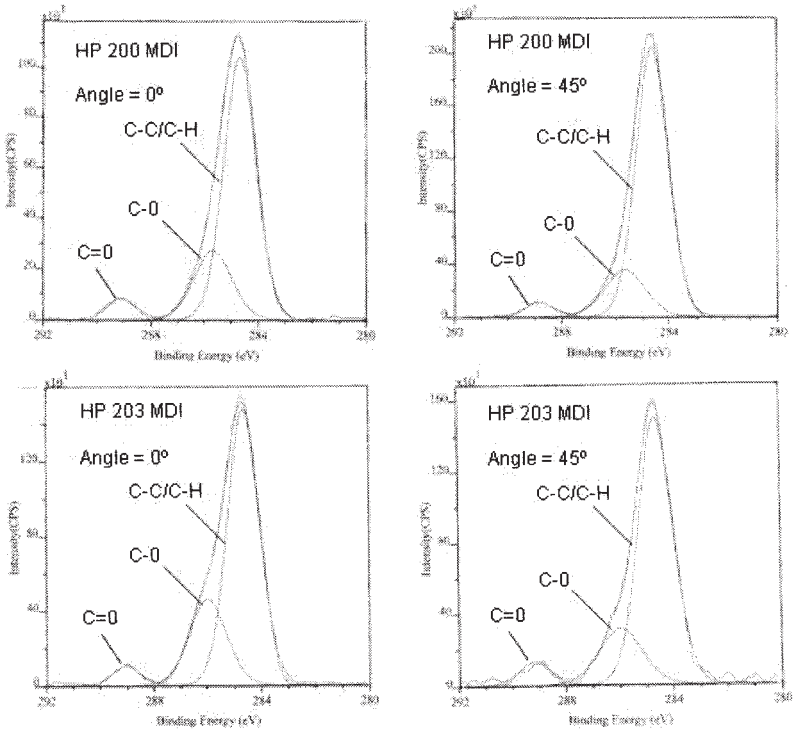

Figure 9 Deconvoluted AR–XPS spectra of HP200MDI and HP203MDI films at takeoff angles of 0 and 45°.

played in Figure 13; we can see that the outer layer was significantly damaged. After the degradation of HP200M, the size of the bright spots increased because of surface oxidation. Defects in some of the films before exposure may have been due to residual solvents during curing (popping). For the melamine-based coatings, the outer layer was significantly damaged upon exposure for 556 h.

CONCLUSIONS

Three different HPs were synthesized with different diols and crosslinked with MDI and HMMM. These HPs were trans-acetoacetylated with a stoichiometric amount of EAA to acetoacetylate 30% of the available hydroxyl groups, which were crosslinked with MDI and HMMM. The free crosslinked films were prepared and subjected to weathering degradation evaluation. The weathered coatings were analyzed with DMTA, XPS, and SEM. A gradual increase in the modulus, T_g, and ν_e was observed for both types of coatings with few exceptions. At different periods of exposure, the coatings showed anomalous behavior because of the complexity of the degradation process. For the PU coatings, a decrease in the urethane concentration toward the

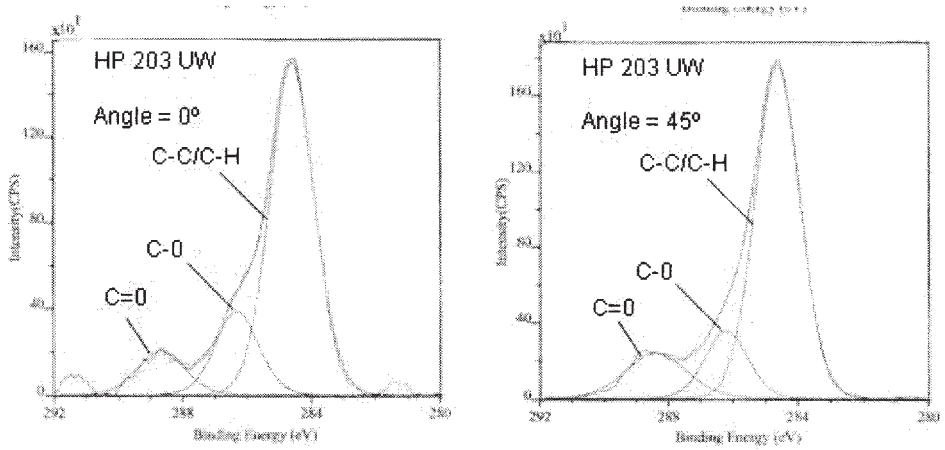

Figure 10 Deconvoluted AR–XPS spectra of urethane-weathered (UW; 556 h) HP203MDI coatings at takeoff angles of 0 and 45°.

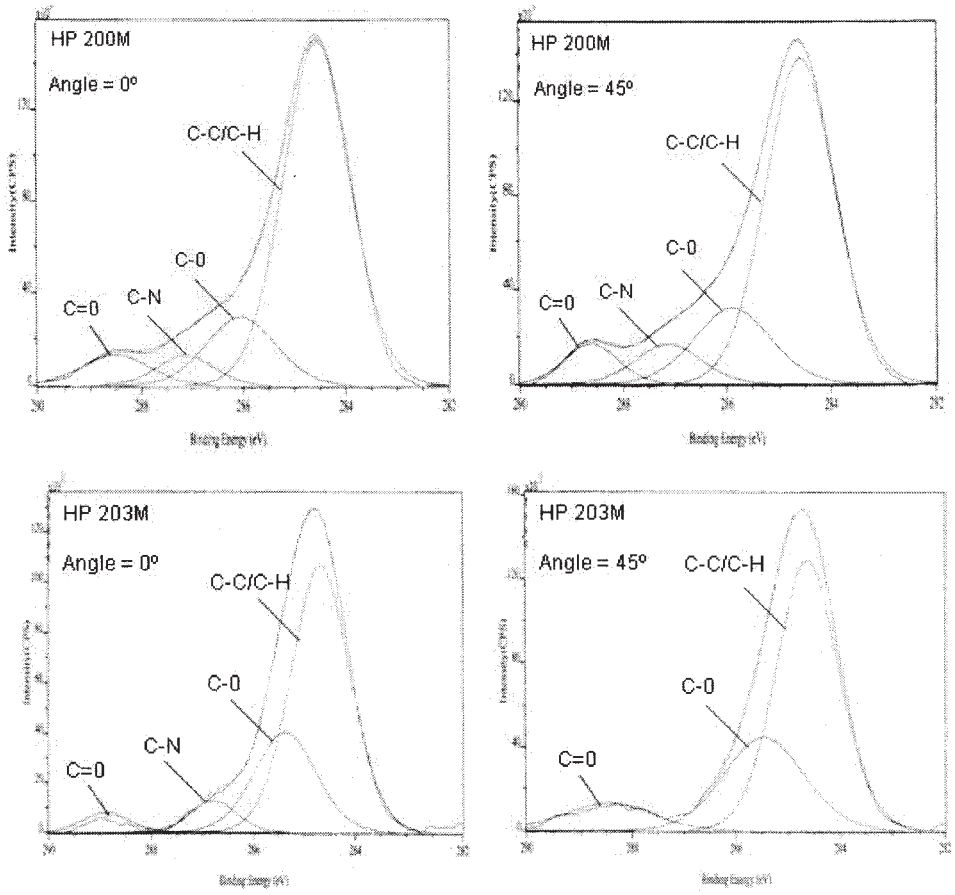

Figure 11 Deconvoluted AR–XPS spectra of unweathered melamine HP200M and HP203M coatings at takeoff angles of 0 and 45°.

coating/air interface was observed, whereas according to XPS spectra recorded at different takeoff angles and after 556 h of weathering; the coating/air interface was enriched with the urethane/urea content. The XPS results showed the surface enrichment of HMMM for the HP200M coatings. The weathered coatings showed a reduction in the melamine content at the surface. SEM analysis showed appreciable damage to the surface upon exposure for up to 550 h for melamine-based coatings. The polyester–

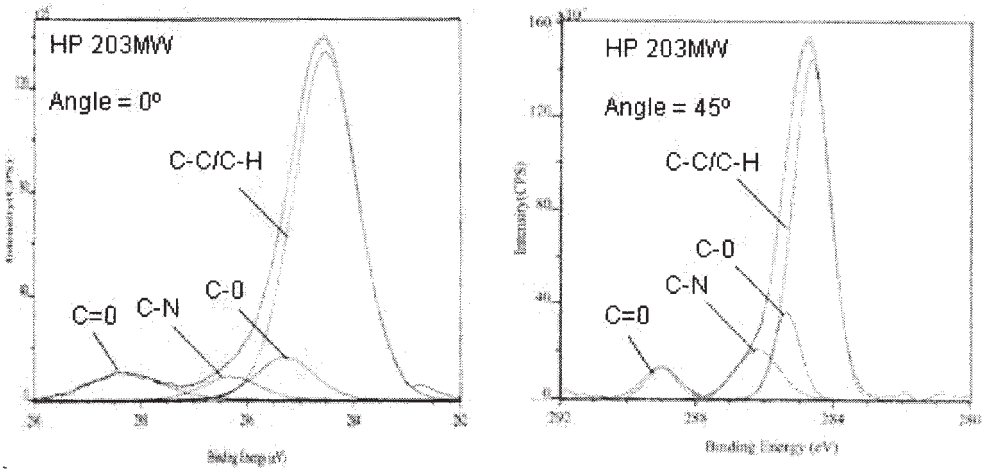

Figure 12 Deconvoluted AR–XPS spectra of weathered (556 h) melamine HP203M coatings at takeoff angles of 0 and 45°.

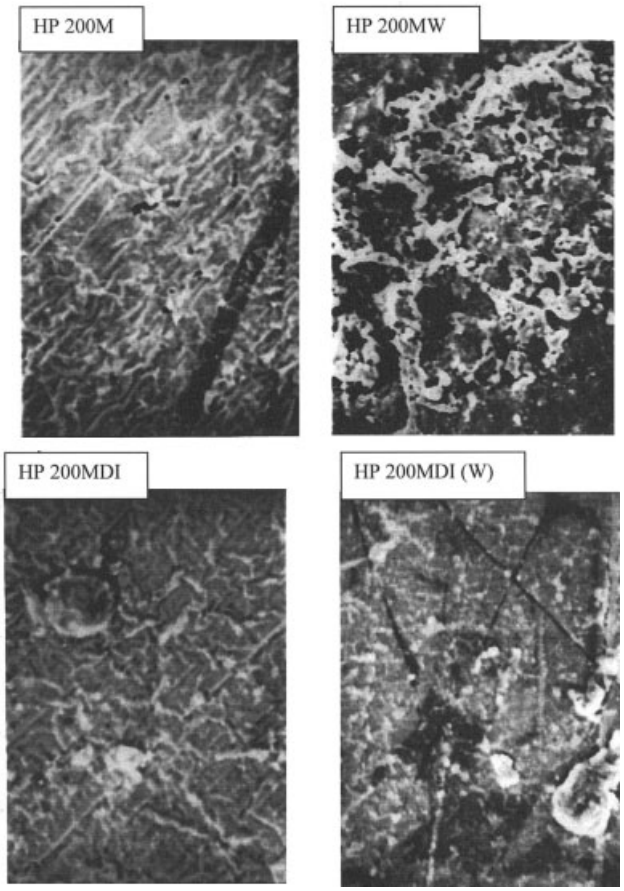

Figure 13 SEM images of HP200M and HP200MDI coatings before and after weathering (556 h).

urethane coatings were more stable toward weathering than the polyester–melamine coatings.

Two of the authors (R.N. and D.K.C.) are grateful to the Council of Scientific and Industrial Research and the University Grants Commission (New Delhi, India) for research fellowships to carry out this research at the Indian Institute of Chemical Technology (Hyderabad, India) under the supervision of K. V. S. N. Raju. This research was a collaborative venture between the Indian Institute of Chemical Technology and the Center of Excellence in Polymer Science (Dharwad, India). One of the authors (N.N.M.) thanks Sanjeev Manohar of the University of Texas at Dallas for his encouragement.

References

1. Yebra, D. M.; Kiil, S.; Johasen, K. D. Prog Org Coat 2004, 50, 75.
2. Yang, X. F.; Vang, C.; Tallman, D. E.; Bierwagen, G. P.; Croll, S. G.; Rohlik, S. Polym Degrad Stab 2001, 74, 341.
3. Yang, X. F.; Li, J.; Croll, S. G.; Tallman, D. E.; Bierwagen, G. P. Polym Degrad Stab 2003, 80, 51.
4. Pickett, J. E. Polym Degrad Stab 2004, 85, 681.
5. Hong, S. G. Polym Degrad Stab 1995, 48, 211.
6. Troev, K.; Tsekova, A.; Tsevi, R. J Appl Polym Sci 2000, 78, 2565.
7. Schmid, E. V. Exterior Durability of Organic Coatings, Survey; UK FMJ International: Publ. Lin. Redhil, 1988.
8. Pappas, S. P. Prog Org Coat 1989, 17, 107.
9. Dickie, R. A. J Coat Technol 1994, 66, 28.
10. Dickie, R. A. J Coat Technol 1992, 64, 61.
11. Simms, J. A. J Coat Technol 1987, 59, 45.
12. Blakey, R. R. Prog Org Coat 1985, 13, 279.
13. Bauer, D. R. J Appl Polym Sci 1982, 27, 3651.
14. Wicks, Z. W.; Jones, F. N.; Peppas, S. P. Organic Coatings Science and Technology; Wiley-Interscience: New York, 1994; Vol. 2, p 132.
15. Yang, X. F.; Tallman, D. E.; Bierwagen, G. P.; Croll, S. G.; Rohlik, S. Polym Degrad Stab 2002, 77, 103.
16. Hill, L. W.; Korzeniowski, H. M.; Andrew, M. O.; Wilson, R. C. Prog Org Coat 1994, 24, 147.
17. Narayan, R.; Chattopadhyay, D. K.; Sreedhar, B.; Raju, K. V. S. N. J Mater Sci 2002, 37, 4911.
18. Davis, A.; Sims, D. Weathering of Polymers; Applied Science: London, 1983; Chapter 10.
19. Ranby, B.; Rabek, J. F. Photodegradation, Photo-Oxidation and Photostabilisation of Polymers, Principles and Application; Wiley-Interscience: New York, 1975; p 242.
20. Wicks, Z. W.; Jones, F. N.; Pappas, S. P. Organic Coatings: Science and Technology, 2nd ed.; Wiley: New York, 1994; Chapter 5.
21. Perrin, F. X.; Irigoyen, M.; Aragon, E.; Vernet, J. L. Polym Degrad Stab 2000, 70, 469.
22. Gardette, J. L.; Lernaire, J. J. J Makromol Chem 1981, 182, 2723.
23. Wilhelm, C.; Gardette, J.-L. Polymer 1998, 39, 5973.
24. Wilhelm, C.; Rivaton, A.; Gardette, J.-L. Polymer 1998, 39, 1223.
25. Hill, L. W.; Kaul, A.; Kozlowski, K.; Santer, J. O. ACS Div PMSE 1988, 59, 283.
26. Biggs, S.; Lukey, C. A.; Spinks, G. M.; Yau, S.-T. Prog Org Coat 2001, 42, 49.
27. Skaja, A. D.; Croll, S. G. Polym Degrad Stab 2003, 79, 123.
28. Narayan, R.; Chattopadhyay, D. K.; Sreedhar, B.; Raju, K. V. S. N.; Mallikarjuna, N. N.; Aminabhavi, T. M. J Appl Polym Sci, to appear.
29. Narayan, R.; Raju, K. V. S. N. Prog Org Coat 2002, 45, 59.
30. Deslands, Y.; Pleizer, G.; Alexander, D.; Santerre, P. Polymer 1998, 39, 2361.
31. Witzeman, J. S.; Nottingham, W. D.; Rector, F. D. J Coat Technol 1990, 62, 101.
32. Bauer, D. R.; Mielewski, D. F. Polym Degrad Stab 1993, 40, 349.
33. Bauer, D. R. Prog Org Coat 1986, 14, 193.
34. Clemens, R. J.; Rector, F. D. J Coat Technol 1989, 61, 83.
35. Decker, C.; Zanouily, K. Polym Degrad Stab 1999, 64, 293.
36. Irusta, L.; Fernandez-Berridi, M. J. Polymer 2000, 41, 3297.
37. Nguyen, T.; Martin, J.; Byrd, E.; Embree, N. Polym Degrad Stab 2002, 77, 1.
38. Otrel, G. Polyurethane Hand Book; Hanser: New York, 1994; p 76.
39. Nielsen, L. E. Mechanical Properties of Polymers; Marcel Dekker: New York, 1974; Vol. 1, p 19.
40. Hill, L. W.; Kozlowski, K. J Coat Technol 1987, 59, 63.
41. Gardette, J. L.; Lemaire, J. J. J Macromol Chem 1982, 183, 2415.
42. Heung, K.; Urbai, M. W. Langmuir 2000, 16, 5782.
43. Gerlock, J. L.; Dean, M. J.; Korniski, T. J.; Bauer, D. R. Ind Eng Chem Prod Res Dev 1986, 25, 449.
44. Wilhelm, C.; Rivaton, A.; Gardette, J. L. Polymer 1998, 39, 1223.
45. Bauer, D. R.; Briggs, L. M.; Labaca, S. S.; Dickie, R. A. Characterization of Crosslinked Polymers; ACS Symposium Series 243; American Chemical Society: Washington, DC, 1984.
46. Kojima, Y.; Sato, T.; Tanuma, T.; Sugitani, H. Adv Org Coat Sci Technol Ser 1991, 13, 297.
47. Gamage, N. J. W.; Hill, D. J. T.; Lukey, C. A.; Pomery, P. J. J Polym Sci Part A: Polym Chem 2004, 42, 83.
48. Hirayama, T.; Urban, M. W. Prog Org Coat 1992, 20, 81.
49. Kanai, H.; Nagase, M.; Futa, M.; Hamada, T.; Koike, T. Tetsu to Hagane 1997, 83, 791.